Assessing accuracy of hindcast spectral content in the estimation of wave energy resource

Yves Perignon, Christophe Maisondieu

Assessing accuracy of hindcast spectral content in the estimation of wave energy resource

Yves Perignon [1], Christophe Maisondieu [2]

[1] *LHEEA Lab., Ecole Centrale de Nantes & CNRS, Nantes, France*

[2] *LCSM, IFREMER, Brest, France*

[1] yves.perignon@ec-nantes.fr

[2] christophe.maisondieu@ifremer.fr

Abstract— **This paper extends the diagnosis on spectral accuracy between measurements and hindcast data initially presented for three measurement locations related to the SEMREV test site in Perignon (2017) to a larger set of measurement stations off the French Atlantic and Channel seaboard. Despite the sensitivity of the response of many marine structures to the frequency content of the forcing, the capabilities of spectral estimations has hardly been investigated for hindcast wave models providing either fully resolved spectra, or, as is more generally the case to this date, parameterized spectra evaluated from integral parameters.**

This work takes advantage of the HOMERE high-resolution public wave hindcast data set [Boudiere et al. (2013)] as well as the Candhis buoy network to perform long-term analysis of wave spectra. The set of frequency spectra available over the whole Channel and Bay of Biscay area provides a proper basis for a detailed study and comparison of their evolution in time. Spectral quantities such as the variance spectral density or wave power are compared with chosen concomitant and collocated in-situ measurement data sets from the Candhis network.

The spectral diagnosis performed confirms and emphasizes the strong site dependency in the accuracy of the sea-states assessment, as well as a regional pattern in the signature of the spectral accuracy of wave energy assessment. Contrarily to first hypothesis, no depth dependency can be accounted as a leading factor of spectral inaccuracies in this dataset. The robustness of the estimation is here confirmed by the low inter-annual variability of the signature when consecutively evaluated on multi year time series. The inaccuracies are shown to be greatly enhanced by extreme sea states in terms of integral wave steepness at some but not all stations. The overall influence of the hindcast accuracy is finally evaluated on the spectral energy yield, which clearly enlightens the epistemic uncertainties associated to a wave energy assessment based only on synthetic data yet fully resolved in frequency.

Keywords— **Waves, buoy, sea states, measurements, modelling, , spectral content, resource assessment.**

I. INTRODUCTION

Over the last decades, North Atlantic coastal European waters have seen a rising number of offshore projects including marine renewable energy projects. In such areas having highly energetic sea-states associated with occurrences of extreme conditions [e.g. Saha et al. (2010)], and even world records of measured significant wave heights [e.g. WMO record [20]], specific concerns are raised about the proper estimation of loads and fatigue on structures or moorings, operability, as well as the resource assessment for the wave energy sector. In an attempt to refine the diagnosis on the accuracy in the estimation of sea states for the latter, many studies have been conducted in the past and mainly based on wave model data validated with in-situ measurement.

Validation of hindcast models usually consists in cross-validation of global parameters such as significant wave height, mean direction and peak or mean period against in-situ data recorded by wave buoys or remote sensing data from satellite observation, using standard estimators of the relative errors. As pointed out in Bietner-Grigersen et al, 2016, such validation based on the sole integral parameters is not sufficient to provide a complete validation of the model data, as it doesn't fully assess the ability of the model to accurately describe the spectral and directional distribution of the wave energy within a sea-state. Yet, this information is of major importance for the design of marine structures and more specifically for the assessment and optimization of Wave Energy Converters [Barret (2008), Saulnier et al. (2011)].

In an attempt to qualify the spectral epistemic error associated with hindcast data, Perignon (2017) proposed a simple but efficient method which was applied to a data set comprised of buoys measurements and of a public hindcast database HOMERE [Boudiere et al. (2013)] providing state of the art fully resolved spectra in time at those same locations. The comparisons conducted were able to challenge and diagnose the hindcast data to measurements conducted in the scope of the marine energy test site SEMREV, which enlightened the concern about the importance of epistemic errors associated to hindcast data at use in wave energy projects. From the spectral signature of the errors inferred and from the increase of relative intensity observed between the off shore station and both moorings on site, it was assumed that the decreasing depth and associated increase of

complexity related to the wave propagation in shallower water could explain the observed behavior.

The aim of the present work is now to extend the previous diagnosis made on a refined hindcast database to a larger set of locations, namely through some stations of the Candhis network database. Underlying HOMERE's specificities are recalled in the second section while characteristics of the set of locations considered in the Candhis Network are described in the third section. A presentation of the diagnosis of spectral accuracy is detailed in a fourth part, and the analysis of its direct application to the set of stations in a fifth. Section six presents an evaluation of the robustness for the spectral signature of the error provided. Then, in an attempt to clarify and refine the domain of inaccuracy of the model, a class analysis is completed on the same dataset. The assessment of the energy yield both measured and modeled is finally compared.

II. HOMERE HINDCAST

The reader is referred to HOMERE's documentation and reference publications [Boudière et al., 2013] for the full description of the setup. For the sake of clarity, we will only recall its main properties. WaveWatchIII® is run in its version 4.09 for the generation of this dataset. HOMERE's domain is dedicated to the whole French Atlantic coastal area from the North Sea to the south of the bay of Biscay. An unstructured grid is built up from triangular meshes over this whole domain. A high-resolution bathymetric database (100 and 500m DTM) provides the reference water depth. Offshore wave conditions are inputted from IOWAGA's global runs over the North Atlantic region. The source terms related to wind input, whitecapping, swell dissipation, and wave breaking are based on Ardhuin et al. (2009a, 2010) formulations (source terms ST4 in WaveWatchIII® v4.18). The non-linear transfers are modeled thanks to the Discrete Interaction Approximation [Hasselmann et al., 1985]. A specific treatment of the bottom friction accounts for the nature of the bottom and for the coupling between sea states and moveable sediments, and coastal reflection is parameterized through a variable reflection coefficient. The spectra are discretized and solved on a 24 directions and 32 frequencies grid.

In terms of forcing, wind conditions are inputed from the 6 hourly CFSR NCEP dataset [Saha et al. (2010)]. Water levels and currents are accounted by tidal constituent inferred from the harmonic analysis of a one-year period (year 2008) hindcast dataset from a multi-rank MARS 2D circulation chain [Pineau-Guillou et al. (2013)].

The HOMERE database includes a large set of global parameters relevant for resource assessment and design studies [Maisondieu (2015), Dubranna (2015), Felice et al, (2015), Perignon & Le Crom(2015)]. A major and original feature of the database is the complementary set of frequency spectra saved at all points of the computational grid which can be of prime interest when assessing the response of a marine structure to the wave loading [Maisondieu & Le Boulluec (2016)].

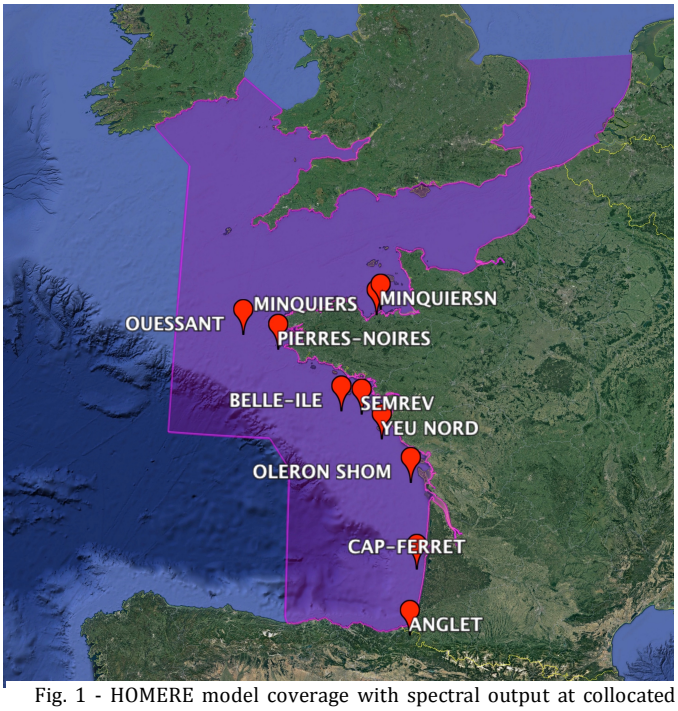

Fig. 1 - HOMERE model coverage with spectral output at collocated and concomitant CANDHIS network of moored wave buoys

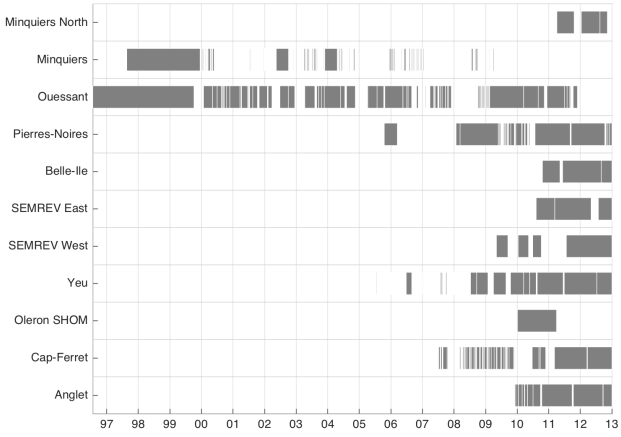

Fig. 2 - Data availability for the 11 measurements from the CANDHIS network, over HOMERE's covered period. Top to bottom: North to South along the coast.

III. CANDHIS NETWORK

The French national network and archive of wave buoy records is managed by CEREMA/CETMEF with complementary local partnerships for financing, deployments and maintenance. In this work, 11 moorings (Fig. 1 and Table 1) are retrieved from the archive for their common coverage in time with HOMERE period (Fig. 2) and for their exposure to North Atlantic wave conditions.

The network comprises standard directional and non-directional Datawell Waverider buoys as well as an experimental lighting buoy (diameter 11.5m, weight 80 tons) equipped with a motion sensor unit from the same manufacturer as the buoy (Datawell). This marine traffic buoy was used at Ouessant, the most offshore mooring in the set of buoys studied hereinafter. Due to its dimensions and inertia, the transfer function in heave of this lighting buoy is indeed advertised by CEREMA to be non-uniform for wave period above 17s and below 4.5s.

The time interval between spectra is not constant through history and can either be 3h, 1h or 30 min depending on the buoy and time in history. The implications of data management and storage in the 90's seem to have been strong enough to limit the output time step to 3h.

IV. Integral and Spectral Diagnosis of Accuracy

The model output are evaluated against buoy measurements in terms of four standard estimators of the relative errors: the normal root mean square error (NRMSE)

$$NRMSE(X)=\sqrt{\frac{\sum\left(X_{obs}-X_{\mathrm{mod}}\right)^2}{\sum X_{obs}^2}} \quad (0),$$

the normalized bias

$$NB(X)=\frac{\sum\left(X_{obs}-X_{\mathrm{mod}}\right)}{\sum X_{obs}} \quad (0),$$

the Pearson correlation coefficient

$$CORR(X)=\frac{\sum\left(X_{obs}-\overline{X}_{obs}\right)\left(X_{\mathrm{mod}}-\overline{X}_{\mathrm{mod}}\right)}{\sqrt{\sum\left(X_{obs}-\overline{X}_{obs}\right)^2\left(X_{\mathrm{mod}}-\overline{X}_{\mathrm{mod}}\right)^2}} \quad (0),$$

and the scatter index (S.I.) correcting NRMSE from its bias

$$SI(X)=\sqrt{\frac{\sum\left[\left(X_{obs}-\overline{X}_{obs}\right)-\left(X_{\mathrm{mod}}-\overline{X}_{\mathrm{mod}}\right)\right]^2}{\sum X_{obs}^2}} \quad (0)$$

all four being dimensionless quantities.

These estimators are classically evaluated for series of integral parameters inferred from the spectral density $E(f)$, such as the variance of the elevation spectrum m_0,

$$m_0=\int E(f)df \quad (0)$$

the associated elevation Hm_0 referred as the significant wave eight H_s

$$H_{m0}=4\sqrt{m_0} \quad (0)$$

the wave energy period Te

$$T_e=\frac{\int f^{-1}E(f)df}{\int E(f)df} \quad (0)$$

or the omnidirectional wave power J

$$J=\int \rho g C_g(f,h)E(f)df \quad (0),$$

with C_g the wave group velocity of a linear wave of frequency f at a local depth h. T_e is retained here among other integral parameters describing properties of the wave periods, such as T_p or T_{m01}, following IEC/TS 62600-101 2015 recommandations for the estimation of the wave energy resource.

The evaluation of the accuracy and comparisons for those four integral parameters actually reflect the integrated influence of the repartition of the error in the spectra. Due to their non-linear relations altogether, those parameters exhibit different properties of accuracy related to the repartition of the spectral error.

In order to evaluate more accurately this spectral accuracy, the previous four estimators of the errors can also be applied directly to spectral quantities. This was depicted in Perignon(2017) through an evaluation of the error on the wave power flux, in frequency. Evaluated at a central frequency f_i and associated bandwidth $2\Delta f_i$ this flux can be expressed as:

$$J(f_i,\Delta f_i)=\int_{f_i-\Delta f_i}^{f_i+\Delta f_i}\rho g C_g(f)E(f)df \quad (0).$$

The independent evaluation of the NRMSE, NB, CORR and SI as a function of f_i provides then a meaningful description of the spectral error. This is notably able to highlight the strong implications of the model accuracy in front of the frequency dependent responses of many structures at sea.

As shown in this former paper, the performance of the wave model seems strongly site dependent. Two collocated moorings on one site (East and West SEMREV, 1km apart) were showing nearly identical signature of the error when Belle-Ile mooring, a more offshore location 40km away, exhibited clear different trends. In an attempt to extend the former evaluation to a larger set of locations, the spectral evaluation is applied here to eight new buoys of the Candhis network complementary to the three previous ones.

As described in this previous work, the comparison process takes advantage of 1D spectral data standardly computed by the buoys but resampled on the HOMERE output frequency grid. This provides a coherent frequency grid for all buoys and model output and allows a proper

	Reference	North Minquiers	Minquiers	Ouessant	Pierres-Noires	Belle-Ile	West SEMREV	East SEMREV	Yeu	Oleron	Cap-Ferret	Anglet
Depth, h	LAT	35m	38m	116m	60m	56m	36m	34m	12m	57m	54m	50m
Mean sea level	[m], Above LAT	5,0	5,2	2,8	3,1	2,5	2,7	2,7	2,6	2,7	2,3	2,3
Latitude	° N (WGS84)	48,99	48,89	48,50	48,29	47,29	47,24	47,24	46,83	46,11	44,65	43,53
Longitude	° E (WGS84)	-2,34	-2,44	-5,80	-4,97	-3,29	-2,79	-2,77	-2,29	-1,59	-1,45	-1,61

Table 1 - Candhis Network, Mooring properties

Quantity	Error, Non-dimensional	North Minquiers	Minquiers	Ouessant	Pierres-Noires	Belle-Ile	West SEMREV	East SEMREV	Yeu	Oleron	Cap-Ferret	Anglet
H_{m0} [m]	NRMSE	0,20	0,17	0,24	0,13	0,12	0,14	0,14	0,12	0,20	0,13	0,16
	CORR	0,95	0,94	0,96	0,97	0,97	0,97	0,97	0,97	0,95	0,97	0,96
	NB	-0,15	-0,03	-0,17	-0,02	-0,01	-0,02	-0,02	-0,03	0,13	0,01	0,05
	SI	0,15	0,17	0,19	0,13	0,12	0,14	0,14	0,12	0,17	0,13	0,15
Te [s]	NRMSE	0,16	0,15	0,12	0,11	0,10	0,22	0,20	0,17	0,23	0,11	0,13
	CORR	0,88	0,89	0,90	0,88	0,91	0,73	0,79	0,88	0,75	0,91	0,90
	NB	-0,10	-0,07	-0,07	-0,05	-0,05	-0,10	-0,10	-0,11	-0,14	-0,06	-0,06
	SI	0,13	0,13	0,09	0,10	0,09	0,19	0,18	0,13	0,19	0,10	0,11
m_0 [m^2]	NRMSE	0,31	0,47	0,58	0,21	0,21	0,26	0,26	0,19	0,34	0,23	0,30
	CORR	0,95	0,82	0,94	0,96	0,96	0,96	0,96	0,97	0,96	0,97	0,96
	NB	-0,26	-0,03	-0,39	-0,02	0,01	-0,06	-0,05	-0,02	0,26	0,07	0,14
	SI	0,26	0,47	0,52	0,21	0,21	0,25	0,26	0,19	0,31	0,22	0,28
J [$W.m^{-1}$]	NRMSE	0,45	0,70	0,89	0,28	0,25	0,33	0,33	0,21	0,33	0,27	0,34
	CORR	0,93	0,64	0,91	0,95	0,96	0,95	0,94	0,97	0,96	0,96	0,95
	NB	-0,44	-0,09	-0,64	-0,08	-0,01	-0,16	-0,15	-0,09	0,16	0,05	0,12
	SI	0,36	0,70	0,83	0,28	0,25	0,33	0,33	0,21	0,32	0,27	0,34

Table 2 – HOMERE's scores compared to Candhis buoys for integral parameters H_{m0}, T_e, m_0 and J.

comparison of wave power flux J on equivalent frequency bands.

V. SITE DEPENDENCY

Applying the four estimators of the error to the four integral parameters either modeled or measured at the eleven locations, one can get a first picture of the local capabilities of the model or for one specific case spot differences in sensor capabilities. The scores computed for the four estimators over the four integral parameters at the eleven selected locations are presented in Table 2 .

As a matter of fact, because of the specificities of the buoy deployed at Ouessant, one should differentiate results obtained at that station from those observed at the other locations equipped with more standard wave buoys. A specific frequency cut-off is applied for Ouessant data above 0.3 Hz in the computation of the parameters inferred from $E(f)$, in agreement with the size of the buoy and the wave periods which can't be retrieved from the buoy heave motion. The score of the model on integral parameters is then worse than the one at more coastal locations contrarily to more classical performances in deep waters [Dodet et al. (2010)]. The strong limitations of the measurement platform are here particularly stringent.

For all other buoys whose comparisons to some HOMERE output data were already included in Boudière et al. (2013)'s reference publication, the estimation of the model for all the parameters seems quite homogenous over the sea front. With the exception of Oleron buoy, all offshore buoys located on sites widely open to the Atlantic influence show the best performances of the model: for instance, their NRMSE remains below 16% on Hm0. Minquiers and SEMREV area are naturally more sheltered either inside the macro tidal Channel Sea (i.e. tidal range above 10m) or in the shadowing of Belle-Ile Island for north west originated sea swells, and they seem to present an added complexity slightly not resolved as well by the model. For some reasons, Oleron is more poorly resolved even if it seemed to share the same off shore properties as Belle-Ile, Cap-Ferret or even Anglet buoys. The bias shows a low overestimation of the significant wave height north of the area, and an underestimation in the south of the Bay of Biscay from Oleron to Anglet. The correlation even remains superior to 94% for all sites on H_{m0}. If correlation on T_e is a bit lower, the overall performance in terms of SI reaches the same order of magnitude as the one on H_{m0}.

Due to their different non-linear dependence to $E(f)$, m_0 and J are clearly less accurately resolved than H_{m0} or T_e for all buoys. Apart from Ouessant, the lowest performance on those quantities is by far recorded at Minquiers. If all buoy measurements are here considered as reference data, this still clearly raises some questions regarding the better performances identified at the other neighboring mooring of North-Minquiers. As previously stated for the NBias on H_{m0}, both the variance of the elevation spectrum and the power flux are underestimated for Oleron and the southern buoys when those quantities are overestimated North of Yeu buoy. An hypothesis related to the length of the continental shelf that most West originated wave systems have to cover could for instance be explored to explain such a discrepancy: the shelf is indeed notably narrower to the south of the Bay of Biscay than to the north. It was also recently analyzed that the Bay of Biscay was experiencing different trends in its climatology from its northern regions to its southern [Maisondieu (2016)]. Such different statistics of the incoming sea states upstream of the continental shelf would play its part in the observed more coastal behavior.

Then, looking at the spectral signature of the errors enables to get a more accurate look at the repartition of any misfit in frequency, concurring to the integral scores just described. The choice is made in this paper to use an integration of power flux by frequency band for the meaning it carries in the wave energy resource

assessment, but the evaluation carried directly on the spectral density still qualitatively preserves the trends that will be described in the following.

As first described in Perignon (2017) at three of those buoys, all eight new locations still show overall clear trends in the spectral signature of the errors (Fig. 3 to Fig. 6). For all locations, the low frequency part below 0.1 Hz is the one showing the maximum error, with NRMSE peaking either at the lowest resolved frequency or at a more intermediate low frequency below 0.07 Hz. In the mean time, CORR drops at the lowest frequencies while NBias shows an underestimation at the same lowest frequencies. For the NBias, this is followed by a maximum overestimation below 0.1 Hz and a return to a plateau for higher frequencies. All in all, no unique trend can be drawn form those spectral comparisons and the site dependency is then confirmed to be a leading factor of uncertainty.

Ouessant station being specific by its sensor, its analysis should again be considered apart from the others. The spectral signature of the error is the clear illustration of the discrepancies observed in the previous section on integral parameters. Here again the observations performed by this buoy are overall the most poorly hindcasted by the model despite the deep-water location of the mooring. It seems that for this location, the limitations in the dynamics of the platform itself play a significant role in the observed inaccuracies and that the model alone is not accountable for the misfit. The increase in NRMSE, BIAS and by definition SI, and decrease of CORR above 0.2 Hz can clearly be related to the size of the floating platform which tends to increase the filtering of the motion above this limit.

Despite the relative vicinity of mooring sites for Minquiers and Minquiers North, the performance of the model at both sites is quite different, confirming the first comments made from integral parameters comparisons. The NRMSE peaks at nearly 100% at the low frequency limit at Minquier, when Minquiers North shows a maximum above 80% at a more intermediate low frequency (~0.07Hz). The CORR drops significantly for Minquiers below 0.1Hz, providing by a great margin the worst performances of all 11 buoys for those frequencies. Minquiers North does not exhibit such a trend on CORR,

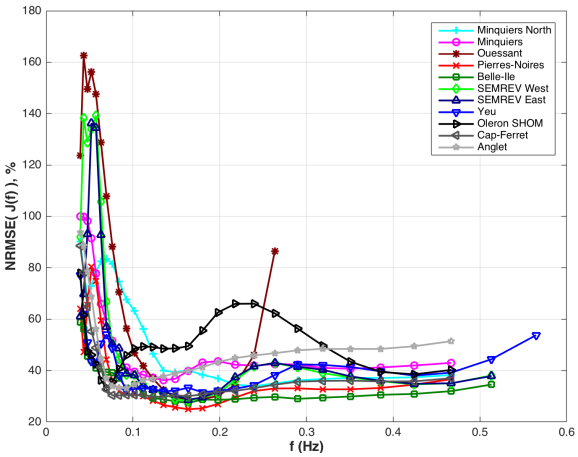

Fig. 3 –Spectral signature of the NRMSE for the 11 buoys

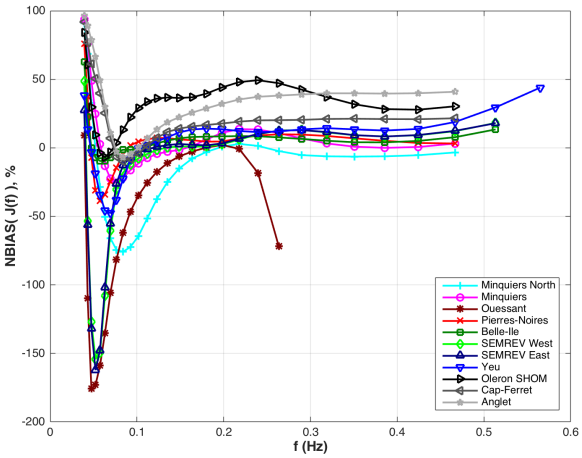

Fig. 5 - Spectral signature of the NBIAS for the 11 buoys

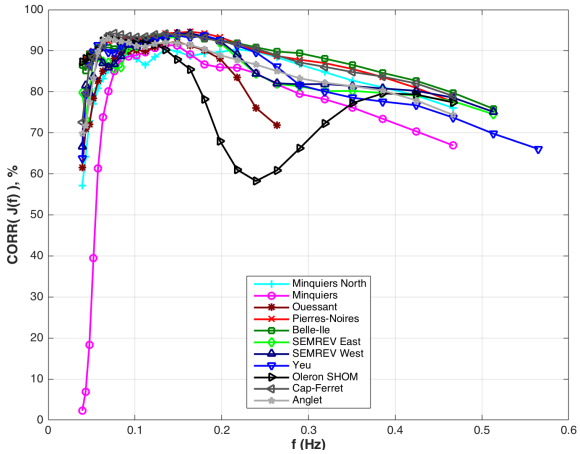

Fig. 4 –Spectral signature of the CORR for the 11 buoys

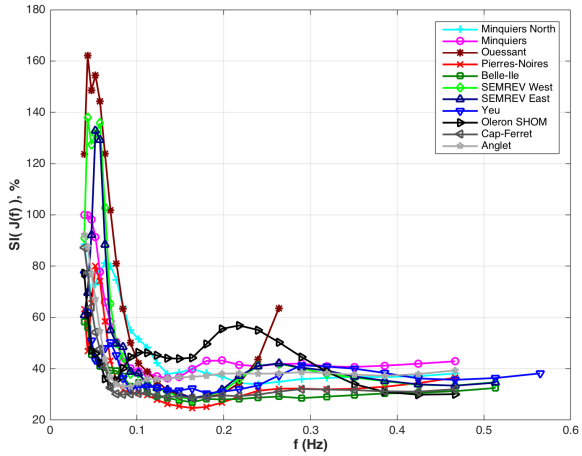

Fig. 6 –Spectral signature of the SI for the 11 buoys

but presents a maximum peak in NBIAS near 0.08 Hz, overestimating the wave power in this spectral area and up to 0.2 Hz.

Pierres-Noires and Belle-Ile measurement sites both show significantly lower errors. Pierres-Noires demonstrates a peak of error at intermediate low frequency in NRMSE, NBIAS and SI which is not present at Belle-Ile, but overall the performances of the model are of the same order of magnitude and more specifically from 0.1 to 0.5Hz.

SEMREV's related measurements at East and West corners of the site, broadly 1km apart, show really close performances despite their differences in time coverage, as already described in Perignon (2017). Compared to other Candhis sites, the peak discrepancies in NRMSE, NBIAS and SI at low frequency are the most significant of all the ten other sites using Datawell Waverider buoys as sensors. The CORR remains on the other hand in the average range of those buoys. The occurrence of a peak error in NRMSE, with a strong overestimation of the resource and still acceptable correlation of the model emphasize the possible impact of a dissipative process mis- or unaccounted for in the energy balance.

Despite its quite shallow water, the site of Yeu remains quite accurately hindcasted by the model. It shows some of the best performances at low frequency in terms of NRMSE and CORR, with a contained BIAS. At higher frequencies, the NRMSE and NBIAS rise a bit with a drop in CORR, which could reflect some local wind-sea effects not properly resolved by the model or its forcing in this coastal area.

Among all three southern stations, Oleron site clearly raises a challenge to the model capabilities. The spectral region which sees the best capabilities of the model with periods comprised in a [3s;12s] interval for all other sites is here significantly not as properly resolved. Instead of dropping at frequencies above 0.08Hz, the NRMSE increases again to a local maximum near 0.22Hz. The CORR significantly drops to 60%, and shows by far the lowest performance at those frequencies among other buoys. Sea states are underestimated nearly over the whole spectral resolved domain, as already suggested by integral results on the bias provided in Table 2.The two other mooring sites, Cap-Ferret and Anglet, share some trends with Oleron's signature but the intensity of the error remains lower at most frequency domains. The best performances are observed at Cap-Ferret site, while Anglet signature reaches Oleron's one above 0.3Hz. The location and increase of the error in frequency could indicate that local wind seas are not properly resolved for those stations with a particular inaccuracy at Oleron for a given frequency band. A directional analysis could easily clarify if the nearly straight coast at Cap-Ferret, or the local channel between Ré and Oleron Island for Oleron station, and associated fetches depending on wind directions could explain the observed discrepancies.

VI. Inter Annual Variability

Error estimators presented on figures 3 to 6 are averaged parameters estimated from long time series corresponding to several years of data. It is then interesting to assess the representativeness of these averaged parameters and the potential variability of the spectral signature of such estimators.

Choice was made to compare the values of these estimators computed from annual datasets so as to assess the sensitivity of the spectral signature of the error to the interannual variability of the sea-states, hence somehow to the local wave climate.

An example of this is given figure 7 presenting the NRMSE of the energy flux assessed at buoy Cap Ferret for each year between 2007 and 2012. A good stability of the spectral shape of the error parameter is observed throughout the years confirming the robustness and representativeness of the spectral signature of the estimator. It is worth noting that the curves departing the most from the average shape, especially in the energetic spectral band between 0.07 Hz and 0.25 Hz are those corresponding to the years with the smallest data coverage (data was available 33% and 43% of the time for years 2007 and 2010 respectively compared to a rate of availability higher than 82% for the other years). This indicates sensitivity to the variability of the instant error evaluation but confirms the representativeness and robustness of the averaged spectral signature. Similar trends are globally observed at the other stations.

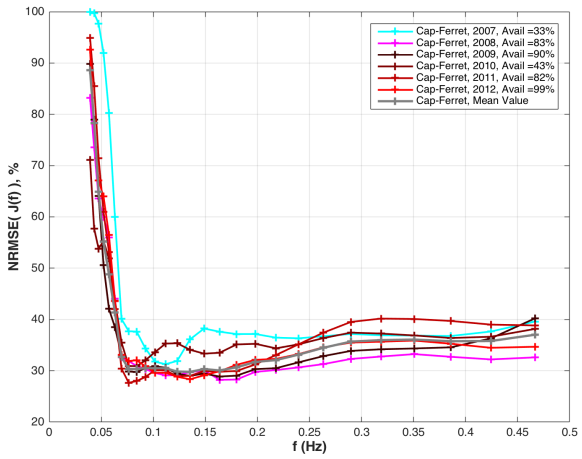

Fig. 7 - Interannual variability of flux energy NRMSE at the Cap-Ferret station

VII. Sea States Dependency

In an attempt to further refine the diagnosis on the model capabilities, it could be of great interest to evaluate the influence of the severity of the sea state or the local spectral content may have on the model capability for any given site.

For such a task, the evaluation previously conducted on $J(f_i,\Delta f_i)$ as expressed in Eq (0) can be achieved for N classes of any control parameter. As a matter of fact, in an attempt to evaluate the severity of the sea states, the steepness $\varepsilon = k_p H_{m0}$ is considered here as such a control parameter over several intervals $I_n, n \in [1,N]$. The evaluation is then conducted here on N samples of $J(f_i,\Delta f_i)$ such as :

$$J_n(f_i,\Delta f_i) = J(f_i,\Delta f_i), \quad \varepsilon \in I_n \qquad (0)$$

Thus each sample of power flux, classified by integral steepness of their associated sea states, sets up an ensemble of sea states on which the performance of the hindcast model can be assessed through their NRMSE, CORR, NB and SI.

Applied to the same 11 former stations, this reveals again some site-specific behavior in the hindcast capabilities. The 2D error maps show different trends in the dependency of the error in ε over the frequency domain, as depicted for instance Fig. 8 for the SI at Pierres-Noires, and Fig. 9 at North-Minquiers. For several stations, the classification on steepness seems able to discriminate a class of conditions for which the error is clearly enhanced, as it is at Pierres-Noires with SI peaking above 400% of error and well above the integral SI plotted Fig. 4. At other stations such as North-Minquiers, a slight dependency of the error is illustrated in steepness and frequency through the non-uniform error map plotted Fig. 9, but the classification in integral steepness does not provide a trend as clear as what is observed at Pierres-Noires. Several tests were conducted with other control parameters than ε, but again no universal classification seems able at this stage to differentiate for all 11 buoys the limiting conditions regarding model performances.

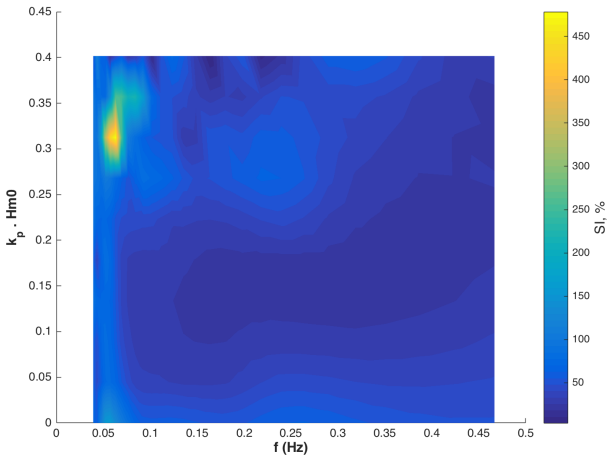

Fig. 8 – Error map of the SI in frequency and by classes of integral steepness at Pierres-Noires station.

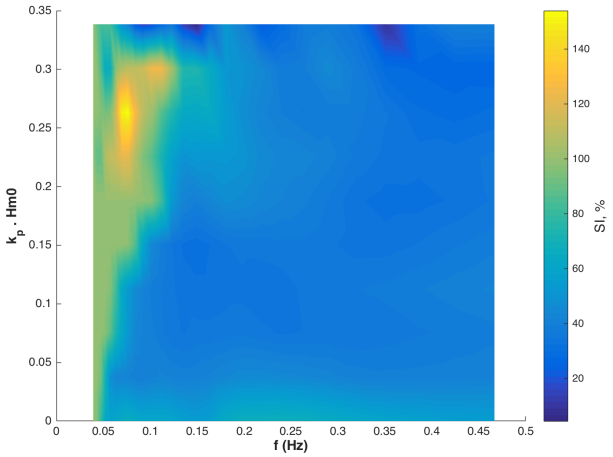

Fig. 9 – Error map of the SI in frequency and by classes of integral steepness at North-Minquiers station

VIII. WAVE ENERGY RESSOURCE

As previously detailed in Perignon(2017) for two Semrev stations and Belle-Ile's one, the spectral bias of the hindcast model accounts for a great portion of the misfit in the estimated cumulated wave energy yield. As confirmed in section V of this paper for a greater number of stations, this spectral bias demonstrates a strong site-dependent behavior. This can be directly illustrated with the assessment of an equivalent mean spectral wave energy resource both from buoy measurements and hindcast database at each measurement site. This provides a direct and meaningful illustration that for wave energy converters whose principles imply a frequency-dependent response and power conversion, the influence of the spectral misfit observed in the resource assessment could be significant.

Ten stations are considered here among the eleven for the sake of clarity. Indeed, the capabilities of Ouessant buoy don't enable a confident estimation of the resource from its measurements; the poor comparisons at this station are clearly a combination of buoy inaccuracy and model inherent error, which cannot be differentiated and whose respective orders of magnitude are not clearly quantified. Fig. 10 illustrates this comparison for the ten retained other stations.

As already described through the evolution of the NBIAS, northern stations see an overestimation of the resource, when sites farther south than Oleron are slightly underestimated by the model. This comparison provides another aspect of the strong site-dependency related to wave resource assessment, as the evaluation of the energy yield is the direct result of cumulated effects studied in the previous sections. The implications of those comparisons are numerous and sometimes specific to the wave energy converter to be deployed. Among generic remarks, one can evaluate that the strong NBIAS observed at Minquiers North lead for instance to a significant overestimation of the resource all around the peak of the available resource.

More over all sites from Minquiers North to Yeu see a downshift in frequency of the peak available resource from buoy to model estimations. An optimal converter deduced from model analysis only would visibly not be optimal if confronted to real conditions more consistent to measurements. An application to realistic test cases of WEC response is for now beyond the scope of this paper, but here again, the spectral estimation of the resource seems to raise some clear questions that might benefit to the current uses and practices.

IX. Conclusions and Discussions

A refined spectral diagnosis has been conducted in this study in order to evaluate the current capabilities of the HOMERE hindcast database compared to measurement data gathered at eleven stations of the CANDHIS French buoy network. After a standard evaluation of its performances in terms of integral parameters, the spectral signature of the hindcast error is ascertained following Perignon (2017) method and preliminary analysis.

First of all, the spectral diagnosis conducted was able to differentiate performances at Ouessant station from all other stations; indeed, the comparisons of model and measurement data from the experimental platform moored at this site clearly exhibited the lowest performances of the whole dataset, which could not be related to usual performances of the model compared to standard offshore buoys. Measurements were not considered above 0.3Hz, which was estimated coherent with the buoy dimensions and the assumed limitations of its hydrodynamic response. Thus for this unique and specific buoy, the epistemic error of the model could not be considered dominant in front of the measurement and sensor uncertainties.

Then, the present study on the ten other stations confirms and emphasizes the strong site dependency of the spectral signature of the error as well as some regional patterns. Apart from nearly collocated measurements at

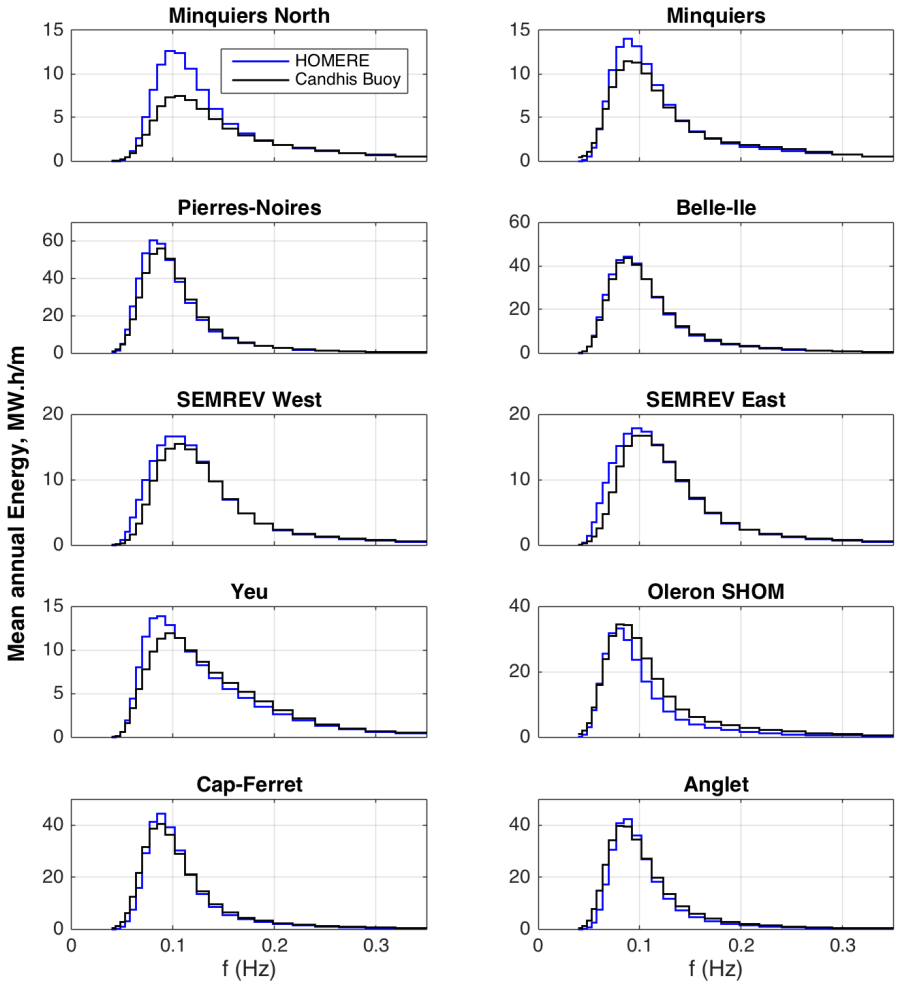

Fig. 10 – Comparison of the mean annual energy yield at eight Candhis stations estimated from measurements and hindcast data

SEMREV test site with identical signatures, each site shows a distinctive pattern. The low frequency part of the spectrum is overall the least properly resolved for all stations, with some specific higher frequency peak errors in the 0.25Hz region for some coastal locations (i.e. Oleron, SEMREV, Yeu, etc.). A slight trend seems to emerge from north to south stations with a general increase of the bias for the hindcast; the model overestimates the low frequency part of the sea states below 0.08Hz north of Yeu and underestimates globally the whole frequency band from Oleron to Anglet stations. Several candidate hypotheses could explain the observed discrepancies, but ad-hoc detailed studies should be conducted in order to evaluate the influence of some assumptions made on the physics currently accounted for in the model.

Taking advantage of several available multi-year measurements, the robustness and representativeness of the spectral signature diagnosed for the Candhis measurement stations is confirmed by a low interannual variability. The weight of extreme events, in terms of integral steepness, in the spectral signature of the errors is also shown to be significant but not predominant and certainly not the unique and leading factor of inaccuracy for every sites.

Finally, the impact of this spectral error on the energy yields, related to the bias previously studied and cumulative properties, is shown to particularly illustrate the strong site dependency of the estimation.

It should be noted that this study is conducted in the spectral domain only, hence doesn't explicitly accounts for the directionality of the wave systems. Directionality may also have some influence, especially in coastal areas and over a domain for which occurrences of complex sea-states are high. The measurement process was assumed ideal except for one experimental buoy, but the measurements themself as well as the behavior of moored buoys in complex hydrodynamic environments may hold a fraction of the uncertainty that is currently only related to the model.

These results reinforce overall the idea that resource assessment based on the sole global parameters is not sufficient and that spectral distributions of the energy should also be accounted for. Site-specific in-situ measurements from field-proven sensors would hence be mandatory to ascertain the local uncertainties induced even from the latest and most refined hindcast chains.

ACKNOWLEDGMENT

The work presented here was supported by LHEEA Lab. at Centrale Nantes, France, in the context of the scientific gathering LabexMer (Program “Investment for the future” grant ANR-10-LABX-19-01) and SEMREV test site. This study was made possible by the use of the CANDHIS national database managed by CEREMA/CETMEF.

REFERENCES

[1] Ardhuin, F., Chapron, B., & Collard, F. (2009). Observation of swell dissipation across oceans. *Geophys. Res. Lett. , 36*.

[2] Ardhuin, F., Rogers, E., Babanin, A. V., Filipot, J.-F., Magne, R., Roland, A., et al. (2010). Semi-empirical Dissipation Source Functions for Ocean Waves. Part I: Definition, Calibration, and Validation. *J. Phys. Oceanogr. , 40* (9), 1917-1941.

[3] Ardhuin, F., Roland, A., Dumas, F., Sentchev, A., Forget, P., Wolf, J., et al. (2012). Numerical wave modeling in conditions with strong currents: dissipation, refraction and relative wind . *J. Phys. Oceanogr. , 42*, 2101-2120..

[4] Barrett, S., Holmes, B., & Lewis, A. (2008). Monitoring of Seaway Variability on WEC Performance. In Proceedings of the 2nd International Conference on Ocean Energy (pp. 1–9). Brest, France.

[5] Bitner-Gregersen, E. M., Dong, S., Fu, T., Ma, N., Maisondieu, C., Miyake, R., & Rychlik, I. (2016). Sea state conditions for marine structures' analysis and model tests. *Ocean Engineering*, *119*, 309-322. http://doi.org/10.1016/j.oceaneng.2016.03.024

[6] Boudiere, E., Maisondieu, C., Ardhuin, F., Accensi, M., Pineau-Guillou, L., & Lepesqueur, J. (2013). A suitable metocean hindcast database for the design of Marine energy converters. *International Journal of Marine Energy , 3-4*, e40-e52.

[7] Dodet, G., Bertin, X., & Taborda, R. (2010). Wave climate variability in the North-East Atlantic Ocean over the last six decades. *Ocean Modeling , 31*, 120-131.

[8] Dubranna, J., Ranchin, T., Ménard, L., & Gschwind, B. (2015, September). Production and Dissemination of Marine Renewable Energy Resource Information. In *11th European Wave and Tidal Energy conference (EWTEC)*, Nantes, France .

[9] Arena, F., Laface, V., Maisondieu, C., Malara, G., Olagnon, M., Nuwolko Komlan, K., Strati, F. M. (2015). On wave energy exploitation by U-OWC devices in the West coast of France. In *11th European Wave and Tidal Energy conference (EWTEC)*, Nantes, France .

[10] Hasselmann, S., & Hasselmann, K. (1985). Computation and parameterizations of the nonlinear energy transfer in a gravity-wave spectrum. Part I: a new method for e*ffi*cient computations of the exact nonlinear transfer. *J. Phys. Oceanogr.* (15), 1369–1377.

[11] Maisondieu, C. (2015). WEC Survivability Threshold and Extractable Wave Power. In *Proc. 11th Eur. Wave Tidal Energy Conf.*

[12] Maisondieu C., Le Boulluec M. (2016). Benefits of using a spectral hindcast database for wave power extraction assessment . *The International Journal of Ocean and Climate Systems* , 7(2), 1-5 . Publisher's official version: http://doi.org/10.1177/1759313116649967, Open Access version: http://archimer.ifremer.fr/doc/00347/45799/

[13] Maisondieu, C. (2016). Caractérisation statistique des conditions d’états de mer multimodales dans le Golfe de Gascogne pour le dimensionnement des structures en mer. *15èmes Journées de l'Hydrodynamique*, 22-24.

[14] Perignon, Y., & Le Crom, I. (2015). Challenging best knowledge to real conditions on the SEMREV marine test site. In *11th European Wave and Tidal Energy conference (EWTEC)*, Nantes, France .

[15] Perignon, Y. (2017). Assessing accuracy in the estimation of spectral content in wave energy resource on the French Atlantic test site SEMREV. *Renewable Energy*.

[16] Pineau-Guillou, L., & al., e. *PREVIMER: Improvement of surge, sea level ans currents modelling.* Ifremer.

[17] Saha, S., & al., (2010). The NCEP Climate Forecast System Reanalysis . *Bul. Amer. Meteor. Soc. , 91* , 1015-1057 .

[18] Saulnier J-B, Clément A, Falcão AF, Pontes T, Prevosto M, Ricci P. "Wave groupiness and spectral bandwidth as relevant parameters for the performance assessment of wave energy converters."*Ocean Eng.*, 38(1), 130-147, 2011.

[19] Tolman, H., & et al. (2014). *User manual and system documentation of WAVEWATCH III version 4.18.* NOAA/NWS/NCEP. Hendrik Tolman .

[20] World Highest Significant Wave Height as measured by a Buoy, WMO, 2016. https://wmo.asu.edu/content/World-Highest-Wave-Buoy.